Biotransformation of selenium in the mycelium of the fungus *Phycomyces blakesleeanus*

Journal:	*Analytical and Bioanalytical Chemistry*
Manuscript ID	ABC-00600-2022.R1
Type of Paper:	Research Paper
Date Submitted by the Author:	n/a
Complete List of Authors:	Zizic, Milan; Institute for multidisciplinary research, Department of Life Sciences Stanic, Marina; Institute for Multidisciplinary Research, University of Belgrade, Department of Life Sciences Aquilanti, Giuliana; Elettra Sincrotrone Trieste SCpA Bajuk-Bogdanovic, Danica; Faculty of Physical Chemistry, University of Belgrade, Branković, Goran; University of Belgrade Institute for Multidisciplinary Research Rodić, Ivanka; University of Belgrade Institute for Multidisciplinary Research Živić, Miroslav; University of Belgrade Faculty of Biology Zakrzewska, Joanna; eInstitute of General and Physical Chemistry, NMR Laboratory
Keywords:	biogenic selenium nanoparticles, Phycomyces blakesleeanus, volatile selenium compounds, selenium biotransformation

Biotransformation of selenium in the mycelium of the fungus *Phycomyces blakesleeanus*

Milan Žižić[1*], Marina Stanić[1], Giuliana Aquilanti[2], Danica Bajuk-Bogdanović[3], Goran Branković[1], Ivanka Rodić[1], Miroslav Živić[4], Joanna Zakrzewska[5]

[1] University of Belgrade, Institute for Multidisciplinary Research, Kneza Višeslava 1, 11030 Belgrade, Serbia

[2] Elettra Sincrotrone Trieste S.C.p.A., Basovizza, Trieste, Italy

[3] Faculty of Physical Chemistry, University of Belgrade, Studentski trg 12-16, 11000 Belgrade, Serbia

[4] University of Belgrade, Faculty of Biology, Studentski trg 12-16, 11000 Belgrade, Serbia

[5] Institute of General and Physical Chemistry, Studentski trg 12-16, 11000 Belgrade, Serbia

[*]Corresponding author:

Milan Žižić

Mailing address: Department for Life Sciences, Institute for Multidisciplinary Research, University of Belgrade, Kneza Višeslava 1, 11030 Belgrade, Serbia

Tel/fax +38111 3555 258; mail: mzizic@imsi.rs

Abstract

Biotransformation of toxic selenium ions to non-toxic species has been mainly focused on biofortification of microorganisms and production of selenium nanoparticles (SeNPs), while far less attention is paid to the mechanisms of transformation. In this study, mycelium of fungus *Phycomyces blakesleeanus* was exposed to selenite (Se^{+4}) to examine its ability to reduce Se^{+4} to nanoparticles, as well as to elucidate the mechanisms of reduction itself. Red coloration and pungent odor that appeared after only a few hours of incubation with 10 mM Se^{+4} indicate formation of SeNPs and volatile methylated selenium compounds. SEM-EDS confirmed pure selenium NPs with an average diameter of 57 nm, which indicates to potentially very good medical, optical and photoelectric characteristics. XANES spectroscopy of mycelium revealed concentration dependent mechanisms of reduction, where 0.5 mM Se^{+4} led to predominant formation of Se-S containing organic molecules, while 10 mM Se^{+4} induced production of biomethylated selenide (Se^{-2}) in the form of volatile dimethylselenide (DMSe) and selenium nanoparticles (SeNPs), with SeNPs/DMSe ratio rising with incubation time. Several structural forms of elemental selenium were detected, predominantly monoclinic Se_8 chains, together with trigonal Se polymer chain, Se_8 and Se_6 ring structures.

Keywords: biogenic selenium nanoparticles, *Phycomyces blakesleeanus,* volatile selenium compounds, selenium biotransformation

Statements and Declarations: The authors have no relevant financial or non-financial interests to disclose.

Introduction

Selenium represents an essential microelement and, as component of selenoproteins is involved in redox homeostasis and redox regulation of intracellular signaling [1]. It can exist in several oxidation states (-2, 0, +4 and +6) that determine its beneficial or detrimental effects in biosystems. In the form of selenide (Se^{-2}), it plays an important metabolic role as a precursor of a number of organic biomolecules such as coenzyme Q, selenocysteine and selenomethionine [2, 3] or can bind to metals to form metal selenides [4]. Selenite (Se^{+4}) and selenate (Se^{+6}) are often toxic due to their water solubility and bioavailability [3, 5]. Tolerance or resistance toward metal(loid)s can be conferred through physico-chemical properties of the environment, decreased uptake or extracellular precipitation by the organism, adsorption to cell wall components, or through biological reduction to a less toxic chemical form such as Se^0 [6] and volatile methylated selenium compounds. Elemental selenium (Se^0) is water insoluble and inert, non-toxic for humans and animals at low concentrations [7]. Aside from detoxification, bioreduction to Se^0 often has the added value of production of elemental selenium-nanoparticles (SeNPs) that have exceptional physical and chemical properties and numerous applications in biomedicine and industry [5, 8, 9]. Chemical and biological activities of SeNPs vary in size-dependent manner, with significantly better antioxidant activity of particles with diameter under 100 nm [10]. Biogenic formation of SeNPs is mainly attributed to, and mostly studied in bacteria, some of which exhibit capacity for production of SeNPs with a diameter range of 30-500 nm [10]. The research of fungal capacity for SeNPs formation is gaining momentum in the last decade [9–13]. Biomethylation of selenide represents a known and promising detoxification mechanism that produces volatile Se compounds such as dimethylselenide (DMSe) or dimethyldiselenide (DMDSe) [13].

The majority of fungi are yet to be tested for their ability of Se^{+4} or Se^{+6} reduction, which is not necessarily correlated to their tolerance for selenium anions [5, 6]. Most fungal species known so far to reduce Se^{+4} require a lot of time for reaching substantial mycelial biomass [9, 14, 15]. *Phycomyces blakesleeanus* is a non-pathogenic filamentous fungus easy to cultivate, characterized by short life cycle and a rich yield of mycelium in a short time [16].

In this research, we examined the capability of *P. blakesleeanus* for Se^{+4} and Se^{+6} reduction, and investigated ways of Se transformation in dependence of concentration and incubation periods.

Materials and Methods

Mycelium cultivation and materials

The wild-type strain of the fungus *P. blakesleeanus* (Burgeff) (NRRL 1555(-)) was used. The mycelium was grown in standard minimal medium [17], with spore concentration of 10^5/ml, in Erlenmeyer flasks which were shaken at 120 rpm in the growth cabinet with continuous overhead white fluorescent light at temperature of 20°C. Fre of growth, mycelium was filter washed and 200 mg of fresh weight (FW) was dissolved in 1 mL of fresh medium supplemented with 0.5, 2 or 10 mM Se^{+4} or Se^{+6} for 24 h.

Scanning Electron Microscopy - Energy Dispersive X-ray Spectroscopy (SEM – EDS)

Mycelium treated with 10 mM Se^{+4} for 24 h was washed twice (4500 x g, 10 min) with 50 mM K-Pi buffer pH=6. Fixation was performed with 3% glutaraldehyde (GA) in the same medium for 30 min at RT, followed by 3% GA fixation overnight at 4°C. Samples were dehydrated in ethanol series (30%, 50%, 70% and 90%) for 1h, chloroform and 100% ethanol for 1h, and then left overnight in 100% ethanol at 4°C. Samples were dried in Critical Point Dryer K850 CPD (Quorum Technologies, UK), sputter coated with gold for 100 sec at 30 mA (Baltec SCD 005) and examined by SEM (JSM-6390LV, JEOL USA, Inc.). Elementary

composition of samples was obtained with energy dispersive spectroscopy (EDS, Oxford Aztec X-max). EDS analysis was conducted on the area of 500 μm^2 per sample.

For SEM-EDS of exudate, mycelium was filter washed and resuspended in deionized water in 1:20 (w/v) ratio and centrifuged at 15000 x g for 10 min to collect exudate of Se^{+4} treated mycelia. Exudate was collected and filtered through 0.22 µm diameter cutoff membrane. Aliquots of 5 µL of exudate were placed on carbon-coated SEM grid and air dried prior to measurements. Samples were mounted to the holder and during measurements were cooled with liquid nitrogen cryo-jet. Electron micrographs were obtained by SEM (Vega TS 5130MM) at voltage of 30V. EDS measurements were performed on 5 different positions from 4 samples chosen based on SeNPs distribution on SEM micrographs.

Dynamic Light Scattering (DLS) spectroscopy

The particle size distribution pattern in exudate was done by Dynamic Light Scattering (DLS) spectroscopy by application of laser light-scattering particle size analyzer (PSA) (Mastersizer 2000; Malvern Instruments Ltd., Malvern, Worchestershire, U.K.). The measurements range of this instrument is from 20 nm to 2 µm. Prior to measurements, all samples were treated in ultrasonic bath for 5 min.

XANES experiments

The mycelium treated with 0.5 and 10 mM Se^{+4} were filtered, washed, and resuspended in deionized water at a ratio of 1:20 (w/v). Aliquots of 5 µL mycelium suspension were placed on 2.5 µm Mylar thin film fixed and attached to the sample holder and freeze-dried overnight. XANES measurements were performed at IAEA X-ray spectrometry experimental station installed at Elettra Sincrotrone Trieste (Trieste, Italy) synchrotron facility [18, 19] . The samples were raster-scanned through the incident X-ray beam with a spot size of 200 µm (h) ×100 µm (v). XANES spectra were acquired in fluorescence mode using a Silicon Drift Detector (SDD) (XFlash 5030, Bruker Nano GmbH, Germany). The spectra of mycelium

were collected in the energy range from 12500 to 12900 eV, with an energy step of 4 eV in pre-edge region, 0.2 eV in edge region and $\Delta k=0.05$ A^{-1} at post-edge region. The experimental spectra were processed by the DEMETER software package [20]. To extract valence information for selenium in mycelium, spectra were compared with those of recorded standards and with literature data.

Raman spectroscopy

The Raman spectra were recorded at the Thermo DXR Raman microscope. Aliquots of 5 μL of control and treated mycelium suspension were placed on the gold plates and measured under the microscope with 50 x magnification, using the 532 nm laser excitation line, with a constant power of 10 mW. The exposition time was 30 s, with 10 exposures, with 900 lines/mm and spectrograph aperture of 50 μm slit. Automatic fluorescence correction was removed by using the OMNIC software (Thermo Fisher Scientific).

For extraction of soluble fraction, filtered and washed mycelium was homogenized with 5 mm stainless steel beads in Tissue Lyser II (Quiagen) with frequency of 30/sec for 1 minute, and then resuspended in potassium phosphate buffer (50 mM, pH 7.2) in 1:2,5 ratio (w/v) . Homogenate was shaken on ice for 30 min. and then centrifuged for 15 min. at 15000 x g. The pellet comprised of larger organelles and cell walls was discarded and supernatant was collected. The remaining organelles and the majority of cell membrane parts were further removed by centrifugation at 100000 x g for 30 min. Obtained soluble fraction was divided into 1 ml aliquots and stored at −80°C until use.

Results and Discussion

The ability of the fungus *P. blakesleeanus* to reduce selenium in anionic forms as selenite (Se^{+4}) and selenate (Se^{+6}) was examined on 28-hour-old mycelium (mid-exponential growth phase), where the reduction process was initially visualized by color changes of the mycelium treated with Se^{+4} or Se^{+6} for 24 h (Fig 1). The mycelium itself is yellow-orange due to

presence of β-carotene [21], so the light red color in 2 mM Se^{+4} treatment is barely visible, but very intense in 10 mM Se^{+4} treatment, indicating the ability of *P. blakesleeanus* for Se^{+4} reduction and formation of amorphous elemental selenium nanoparticles (Fig 1a). The addition of 10 mM Se^{+4} led to a change in color to reddish yellow within 1-2 h. A pungent odor from treated samples indicated the formation of volatile selenium compounds. After 24 h of incubation with 2 mM and 10 mM Se^{+4}, mycelium was separated from growth medium by centrifugation (Fig 1b) and then washed in sterile deionized water 3 times (Fig 1c). Intense red color of the washed mycelium suggests either intracellular reduction and SeNP formation, or SeNP formation adjacent to the cell wall. Pale red color of the first supernatant may originate from SeNPs released through cell lysis or detachment from the cell wall. To test for reactions with components of the medium and exudate (Fig 1d), 10 mM Se^{+4} was added to fresh medium (M), medium filtered after 28 h of fungal growth (F) and boiled 28 h old mycelium (BM) and incubated for 7 days. No visible reduction occurred without the contact of Se^{+4} with live mycelium, indicating its necessity for SeNP synthesis. Mycelium treated with 10 mM Se^{+6} did not change color compared to control for up to 7 days of treatment (results not shown).

Elemental selenium can be produced intra- or extracellularly, with extracellular formation being especially interesting as the particles can be collected without the additional steps of cell lysis [12], while intracellular synthesis of SeNPs prevents migration of Se through water and soil [22]. Pale red color of supernatant in Fig 1c suggests presence of extracellular SeNPs which was further confirmed by SEM – EDS (Fig 2). EDS microanalysis of mycelium suspension and exudates showed characteristic Se signals at 1.4 (SeLα), 11.2 (SeKα) and 12.5 (SeKβ) keV [23, 24], and in addition to carbon and oxygen, measurable amounts of potassium and phosphorous from the wash buffer were detected in the mycelium (Fig 2a down). The

signal of selenium in exudate is practically devoid of any other signals belonging to cellular components (Fig. 2b down).

The size of SeNPs in exudate of mycelium incubated with Se^{+4} for 24 h was measured by DLS (Fig. 3). Diameters of all SeNPs were in the range of 32-95 nm, with an average value of 57 nm. Although the term 'nanoparticles' should be limited to particles with one of dimension up to 1 μm, biogenic SeNPs smaller than 200 nm, that are of particular importance for their biological activity, are found rarely [25, 26]. The size of nanoparticles plays a significant role in their biological activity [27] as the likelihood of interaction with the target system increases with the surface area, so SeNPs produced by *P. blakesleeanus* with the size range of 32-95 nm are worthy of further research.

X-ray absorption near edge structure (XANES) spectroscopy is a suitable method to study physico-chemical properties of atoms in biological systems, and was used to examine the oxidation states and related symmetry of vanadium in *P. blakesleeanus* [28]. Therefore, the process of Se^{+4} transformations in the mycelium of *P. blakesleeanus* was monitored by synchrotron based XANES spectroscopy by using different Se^{+4} concentrations and incubation times (Fig 4). Concentration of 0.5 mM Se^{+4} (low) was chosen for monitoring pathway of reduction with no visible SeNPs synthesis, while 10 mM Se^{+4} (high) induced abundant SeNPs production.

The spectrum of mycelium incubated 24 h in 0.5 mM Se^{+4} reveals reduction of Se^{+4}, indicated by red shift of absorption edge with regard to Se^{+4} standard. (Fig 4a). Since the energy values of absorption edge of Se^{+2}, Se^{+1} and Se^{0} are similar and not unequivocally separated, exact oxidation form cannot be determined this way. However, the post-edge region contains additional peak at 12667 eV (Fig 4a), typical for XANES of RSSeSR containing organic molecules [29, 30]. Yu et al. (2018) have found that sulfhydryl sites of bacterial cell envelope promote Se^{+4} reduction to neutral RSSeSR compounds that can be more easily transported

across cell membrane. On the other hand, production of Se_nS_{8-n} (monoclinic Se^0) form is reflected in similar spectral fashion [22]. The derivative spectrum confirms sulfur (S) as the atom in the first coordination sphere of Se (Fig 4b), with characteristic trough that discerns these from Se^0 derivative [29, 31]. Even though the results are more indicative of Se-S containing organic molecules, at this point we cannot exclude presence of Se-C bond containing metabolites such as Se-Methionine and/or Se-Cysteine, particularly having in mind the ratio in the intensities of the main peak and the peak at 12667 eV [32]. Reduction of 0.5 mM Se^{+4} was monitored in time (Fig 4c), and it is shown that already after 1 h, contribution of Se^{+4} decreased considerably, while after 3 h it could no longer be detected.

As color changes are clearly visible in samples incubated in 10 mM Se^{4+} we ran XANES with high Se concentration for three aforementioned incubation periods. Fig 4d shows XANES spectra of mycelium incubated in 10 mM Se^{+4} for 24 h. The shoulder at 12658.5 eV appeared as a new component in spectrum (Fig 4d insert), indicating reduced form of Se different from those produced in samples treated with lower Se^{+4} concentration [30]. Unlike other elements, the position of Se K lines does not state unequivocally of the oxidation state of Se, but as Se^0 edge is most red shifted among all Se forms and compounds [33], it could indicate that this shoulder originates from elemental red selenium, whose presence was visually confirmed. The main peak of the spectrum positioned at 12663 eV can originate from methylated selenide (Se^{-2}) compounds. It has been published that these volatile compounds represent the product of selenium metabolism in some bacterial [34–36], fungal [6, 37, 38] and microalgal [39, 40] species. Its main edge energy is positioned between the values typical for Se^0 and Se^{+4} [34, 36], with distances that fully correspond to those obtained in the paper of Van Fleet-Stalder for dimethyl selenide (DMSe), Se^0 and Se^{+4}. The corresponding first derivative spectra clearly confirm the observed energy separations (Fig 4e), and comparison with DMSe standard gave a good match (Fig 4e). As volatilization in the form of pungent odor was observed during

incubation of *P. blakesleeanus* mycelium with Se^{+4}, DMSe, together with red Se^{0} in the form of SeNPs, is likely to be the product of Se^{+4} reduction. XANES of the sample incubated for 1 h with 10 mM Se^{+4} showcases that Se^{+4} is completely removed and transformed into two far less toxic forms, Se^{0} and Se^{-2} (Fig 4f). The first derivative spectra establish predominance of methylated Se^{-2} form, but Se^{0}/Se^{-2} ratio gradually rises with time (Fig 4f).

Interesting observation from these experiments was that when Se^{+4} in low concentration was added, this form was still present after 1h (Fig 4c), suggesting that Se transformation is faster with high Se^{+4} concentration, i.e., different, or additional mechanisms are employed.

No changes have been observed in the spectra of the mycelium treated with 10 mM Se^{+6}, suggesting that the mycelium does not have a capacity for its transformation. This is in collision with previous work of Lindblow-Kull [41] who has shown synthesis of selenobiotin by *P. blakesleeanus* with the addition of Se^{+6}, albeit different medium and culture conditions were applied.

Elemental selenium can appear in several crystal allotropes, as monoclinic, trigonal, vitreous, amorphous and cubic [22, 42]. Structural arrangement of Se atoms in SeNPs produced by *P. blakesleeanus* mycelium treated with 10 mM selenite for 24 h was studied by Raman spectroscopy. The most intensive band at 255 cm^{-1} (low-wavenumber spectral region, characteristic for vibrational bands of SeNPs [43, 44] (Fig. 5a) corresponds to symmetric stretching vibration of Se-Se bond, implying production of monoclinic eight-membered single-chain selenium (Se_8) [43–45]. However, deviation from regular Lorentzian shape and broadening points to overlapping of more than one band in this region, implying existence of amorphous form of SeNPs [46]. The shoulder at around 236 cm^{-1} indicates formation of trigonal Se as it derives from a combination of symmetric and antisymmetric stretching vibrations of trigonal structured Se polymer helix chain [43, 46]. The obtained band is a result of E and A1 vibration of aforementioned structural unit [47]. In addition, two most common

allotropes of crystalline SeNPs induce appearance of vibrational bands at 233 and 251 cm^{-1} for trigonal polymeric chain and Se_8 chain structures, respectively [48]. The wavenumbers of these two lines in the spectrum of *P.blakesleeanus* are shifted toward higher wavenumbers (236 and 255 cm^{-1}), and according to Brodsky (1972), this shift along with broad signal could further indicate high degree of disorder in the amorphous structure produced by altered intermolecular interactions [49]. Less ordered amorphous structure induced by polymerization process has been also noted for the next chalcogen, sulfur [46]. Shoulder at high-wavenumber side of the main peak could be attributed to vibrational band of Se_8 ring structures [43], so to clarify, we performed deconvolution of group of signals around 255 cm^{-1} (Fig. 5b). Two bands of lower intensity centered at 268 and 274 cm^{-1} were detected (Fig. 5b). The band at 268 cm^{-1} is attributed to E2 bending vibration of eight-membered elemental selenium [50]. The latter is assigned to the symmetric stretching vibration of six-membered Se ring [43].These results are in some extent similar to those obtained from the Se^{+4} reduction in bacterial strain of *B. selenitireducens* [44] but with a considerably higher partake of chain-like structure of Se_8 nanoparticles whose band is centered at 255 cm^{-1}. Remarkably broader corresponding band has been obtained in the bacterial strain of *A. thiophylum*, which was interpreted as an existence of the amorphous SeNPs [47]. Such explanation should be taken with a caution, as broadening may also be assigned to considerably large size of NPs [51], However, as already mentioned, the appearance of low-wavenumber signal centered at around 236 cm^{-1} from the Se^{+4} incubated mycelium of *P. blakesleeanus* strongly indicates production of amorphous SeNPs [52].

Raman measurements of cellular soluble fraction did not detect any observable signal in the region of SeNPs (Fig. 5a), but broad band with low intensity at 354 cm^{-1}, not observed in the whole mycelium spectrum, most probably derived from the intracellular interaction between Se and sulfur containing protein components [53]. The identical band has been detected in

bacterial strain *Azospirillum brasilense* where formation of Se_6S_2 has been proposed [22]. Since EDX spectra of exudate with SeNPs indicate pure selenium nanoparticles, it is possible that the reduction pathway of Se^{+4} includes Se-S clusters [54]. Selenate/selenite reduction mechanisms seem to be strain specific, but one of proposed mechanisms includes interaction of selenite with sulfur containing tripeptide glutathione in bacteria *Rhodospirillum rubrum* and *E. coli* in the form of selenodiglutathione [5, 23]. The existence of this compound was confirmed in fungal endophyte *Alternaria tenuissima* when exposed to both Se^{+4} and Se^{+6} [55].

Raman spectroscopy of Se^{+6} treated mycelium did not yield results that differed from the control, confirming that *P. blakesleeanus* mycelium cannot reduce extracellularly added Se^{+6} to SeNPs under the given experimental conditions. This could be expected to some extent, having in mind that *P. blakesleeanus* is an aerobic fungus. The same has been documented for various aerobic bacterial and fungal strains where no activity of selenite reductase has been established [10]. Biogenic reduction of Se^{+6} is, mostly, linked to dissimilatory reduction, with Se^{+6} being terminal electron acceptor [56, 57].

The "essential toxin" [1], selenium, is not essential for most fungi, and therefore it can be assumed that their selenium metabolism is primarily focused on detoxification. This is most likely the case for *P. blakesleeanus*, judging by the presence of SeNPs on the outside of the cell wall, and synthesis of volatile DMSe. However, Raman spectra of cytosol extract tell us that *P. blakesleeanus* internalizes Se^{+4}, and its transformation begins intracellularly, where it interacts with S containing organic molecules, or initiates formation of Se_nS_{n-2} NPs. This is supported by the XANES spectra of mycelium incubated with low Se^{+4} concentrations. As EDS suggests pure SeNPs, interaction with S containing organic molecules as a part of Se reduction pathway is more likely. In yeast, and most other organisms, further transformations of selenodithiols leads to Se^0 and H_2Se, a major intermediate metabolite involved in the

synthesis pathway of all forms of selenium occurring in microbial cells, including DMSe [58]. However, a number of pathways for biomethylation of selenium have been suggested to date, including a four step Challengers pathway via methane selenonic acid [54]. Doran [59] proposed a scheme where methylation of inorganic Se by soil *Corynebacterium* involved the reduction of SeO_3- to Se^0 and then a reduction to the selenide. The selenide is then methylated to form DMSe. Rise in Se^0/DMSe ratio with time in 10 mM Se^{+4} incubated mycelium could be a simple consequence of DMSe evaporation while Se^0 concentration rises, but also, rise in insoluble Se^0 concentration makes it more difficult to access for enzymatic metilation [39]. On the other hand, *Alternaria tenuissima* can convert C-Se-C to S^0 [55].

In conclusion, our work has shown that Zygomycetous fungus *Phycomyces blakesleanus* can transform soluble toxic selenite to insoluble innocuous SeNPs and volatile DMSe. The transformation is at least partially intracellular via selenodithiols such as seleno-diglutathione or seleno-dicysteine. The precise position of DMSe first inflection point in XANES derivative spectrum was identified at 12661 eV, and its presence was confirmed by comparison with spectra of DMSe standard. The dimensions of the obtained nanoparticles promise great biological potential and are therefore worth further research.

Acknowledgment: This work was supported by the Ministry of Education, Science and Technological Development of Republic of Serbia, Contracts no. 451-03-68/2022-14/200053; 451-03-68/2022-14/200051; 451-03-68/2022-14/ 200178. XANES experiment was conducted in the frame of the user proposal number 20200229 at XRF beamline at Elettra synchrotron facility and funded by the International Atomic Energy Agency (IAEA). Authors are grateful dr Smilja Marković, Institute of Technical Sciences, Serbian Academy of Sciences, for DLS measurements.

References

1. Lenz M, Lens PNL (2009) The essential toxin: The changing perception of selenium in environmental sciences. Sci Total Environ 407:3620–3633. https://doi.org/10.1016/j.scitotenv.2008.07.056

2. Butler CS, Debieux CM, Dridge EJ, Splatt P, Wright M (2012) Biomineralization of selenium by the selenate-respiring bacterium Thauera selenatis. Biochem Soc Trans 40:1239–1243. https://doi.org/10.1042/BST20120087

3. Perrone D, Monteiro M, Nunes JC (2015) CHAPTER 1 The Chemistry of Selenium. In: Selenium: Chemistry{,} Analysis{,} Function and Effects. The Royal Society of Chemistry, pp 3–15

4. Nancharaiah Y V., Lens PNL (2015) Ecology and Biotechnology of Selenium-Respiring Bacteria. Microbiol Mol Biol Rev 79:61–80. https://doi.org/10.1128/mmbr.00037-14

5. Wadhwani SA, Shedbalkar UU, Singh R, Chopade BA (2016) Biogenic selenium nanoparticles: current status and future prospects. Appl Microbiol Biotechnol 100:2555–2566. https://doi.org/10.1007/s00253-016-7300-7

6. Gharieb MM, Wilkinson SC, Gadd GM (1995) Reduction of selenium oxyanions by unicellular, polymorphic and filamentous fungi: Cellular location of reduced selenium and implications for tolerance. J Ind Microbiol 14:300–311. https://doi.org/10.1007/BF01569943

7. Khubulava S, Chichiveishvili N, Shavshishvili N, Mulkijanyan K, Khodeli N, Jangavadze M, Tsagareli Z, Dgebuadze M, Phichkhaia G (2019) Effect of High Dose of Selenium Nanoparticles on Alimentary Tract in Rodents. J Nanomed Nanotechnol

10:2–5. https://doi.org/10.35248/2157-7439.19.10.531

8. Fesharaki PJ, Nazari P, Shakibaie M, Rezaie S, Banoee M, Abdollahi M, Shahverdi AR (2010) Biosynthesis of selenium nanoparticles using Klebsiella pneumoniae and their recovery by a simple sterilization process. Brazilian J Microbiol [publication Brazilian Soc Microbiol 41:461–466. https://doi.org/10.1590/S1517-838220100002000028

9. Zhang H, Zhou H, Bai J, Li Y, Yang J, Ma Q, Qu Y (2019) Biosynthesis of selenium nanoparticles mediated by fungus Mariannaea sp. HJ and their characterization. Colloids Surfaces A Physicochem Eng Asp 571:9–16. https://doi.org/10.1016/j.colsurfa.2019.02.070

10. Avendaño R, Chaves N, Fuentes P, Sánchez E, Jiménez JI, Chavarría M (2016) Production of selenium nanoparticles in Pseudomonas putida KT2440. Sci Rep 6:1–9. https://doi.org/10.1038/srep37155

11. Zare B, Babaie S, Setayesh N, Shahverdi AR, Shahverdi A (2013) Isolation and characterization of a fungus for extracellular synthesis of small selenium nanoparticles Extracellular synthesis of selenium nanoparticles using fungi. Nanomed J 1:13–19

12. Liang X, Perez MAMJ, Nwoko KC, Egbers P, Feldmann J, Csetenyi L, Gadd GM (2019) Fungal formation of selenium and tellurium nanoparticles. Appl Microbiol Biotechnol 103:7241–7259. https://doi.org/10.1007/s00253-019-09995-6

13. Sabuda MC, Rosenfeld CE, DeJournett TD, Schroeder K, Wuolo-Journey K, Santelli CM (2020) Fungal Bioremediation of Selenium-Contaminated Industrial and Municipal Wastewaters. Front Microbiol 11:. https://doi.org/10.3389/fmicb.2020.02105

14. Espinosa-Ortiz EJ, Gonzalez-Gil G, Saikaly PE, van Hullebusch ED, Lens PNL (2015)

Effects of selenium oxyanions on the white-rot fungus Phanerochaete chrysosporium. Appl Microbiol Biotechnol 99:2405–2418. https://doi.org/10.1007/s00253-014-6127-3

15. Vetchinkina E, Loshchinina E, Kursky V, Nikitina V (2013) Reduction of organic and inorganic selenium compounds by the edible medicinal basidiomycete Lentinula edodes and the accumulation of elemental selenium nanoparticles in its mycelium. J Microbiol 51:829–835. https://doi.org/10.1007/s12275-013-2689-5

16. Žižić M, Živić M, Maksimović V, Stanić M, Križak S, Antić TC, Zakrzewska J (2014) Vanadate influence on metabolism of sugar phosphates in fungus Phycomyces blakesleeanus. PLoS One 9:. https://doi.org/10.1371/journal.pone.0102849

17. Sutter RP (1975) Mutations affecting sexual development in Phycomyces blakesleeanus. Proc Natl Acad Sci USA 72:127–130. https://doi.org/10.1073/pnas.72.1.127

18. Karydas AG, Czyzycki M, Leani JJ, Migliori A, Osan J, Bogovac M, Wrobel P, Vakula N, Padilla-Alvarez R, Menk RH, Gol MG, Antonelli M, Tiwari MK, Caliri C, Vogel-Mikuš K, Darby I, Kaiser RB (2018) An IAEA multi-technique X-ray spectrometry endstation at Elettra Sincrotrone Trieste: Benchmarking results and interdisciplinary applications. J Synchrotron Radiat 25:189–203. https://doi.org/10.1107/S1600577517016332

19. Jark W, Eichert D, Luehl L, Gambitta A (2014) Optimisation of a compact optical system for the beamtransport at the x-ray fluorescence beamline at Elettra for experiments with small spots. Adv X-Ray/EUV Opt Components IX 9207:92070G. https://doi.org/10.1117/12.2063009

20. Ravel B, Newville M (2005) ATHENA, ARTEMIS, HEPHAESTUS: Data analysis for X-ray absorption spectroscopy using IFEFFIT. J Synchrotron Radiat 12:537–541.

https://doi.org/10.1107/S0909049505012719

21. Mehta BJ, Salgado LM, Bejarano ER, Cerdá-Olmedo E (1997) New mutants of Phycomyces blakesleeanus for β-carotene production. Appl Environ Microbiol 63:3657–3661. https://doi.org/10.1128/aem.63.9.3657-3661.1997

22. Vogel M, Fischer S, Maffert A, Hübner R, Scheinost AC, Franzen C, Steudtner R (2018) Biotransformation and detoxification of selenite by microbial biogenesis of selenium-sulfur nanoparticles. J Hazard Mater 344:749–757. https://doi.org/10.1016/j.jhazmat.2017.10.034

23. Kessi J, Hanselmann KW (2004) Similarities between the abiotic reduction of selenite with glutathione and the dissimilatory reaction mediated by Rhodospirillum rubrum and Escherichia coli. J Biol Chem 279:50662–50669. https://doi.org/10.1074/jbc.M405887200

24. Cremonini E, Zonaro E, Donini M, Lampis S, Boaretti M, Dusi S, Melotti P, Lleo MM, Vallini G (2016) Biogenic selenium nanoparticles: characterization, antimicrobial activity and effects on human dendritic cells and fibroblasts. Microb Biotechnol 9:758–771. https://doi.org/10.1111/1751-7915.12374

25. Dwivedi S, AlKhedhairy AA, Ahamed M, Musarrat J (2013) Biomimetic Synthesis of Selenium Nanospheres by Bacterial Strain JS-11 and Its Role as a Biosensor for Nanotoxicity Assessment: A Novel Se-Bioassay. PLoS One 8:1–10. https://doi.org/10.1371/journal.pone.0057404

26. Prasad KS, Patel H, Patel T, Patel K, Selvaraj K (2013) Biosynthesis of Se nanoparticles and its effect on UV-induced DNA damage. Colloids Surfaces B Biointerfaces 103:261–266. https://doi.org/10.1016/j.colsurfb.2012.10.029

27. Peng D, Zhang J, Liu Q, Taylor EW (2007) Size effect of elemental selenium nanoparticles (Nano-Se) at supranutritional levels on selenium accumulation and glutathione S-transferase activity. J Inorg Biochem 101:1457–1463. https://doi.org/10.1016/j.jinorgbio.2007.06.021

28. Žižić M, Dučić T, Grolimund D, Bajuk-Bogdanović D, Nikolic M, Stanić M, Križak S, Zakrzewska J (2015) X-ray absorption near-edge structure micro-spectroscopy study of vanadium speciation in phycomyces blakesleeanus mycelium. Anal Bioanal Chem 407:7487–7496. https://doi.org/10.1007/s00216-015-8916-7

29. Yu Q, Boyanov MI, Liu J, Kemner KM, Fein JB (2018) Adsorption of Selenite onto Bacillus subtilis: The Overlooked Role of Cell Envelope Sulfhydryl Sites in the Microbial Conversion of Se(IV). Environ Sci Technol 52:10400–10407. https://doi.org/10.1021/acs.est.8b02280

30. Weekley CM, Shanu A, Aitken JB, Vogt S, Witting PK, Harris HH (2014) XAS and XFM studies of selenium and copper speciation and distribution in the kidneys of selenite-supplemented rats. Metallomics 6:1602–1615. https://doi.org/10.1039/c4mt00088a

31. Ruiz-Fresneda MA, Eswayah AS, Romero-González M, Gardiner PHE, Solari PL, Merroun ML (2020) Chemical and structural characterization of SeIVbiotransformations by: Stenotrophomonas bentonitica into Se0nanostructures and volatiles Se species. Environ Sci Nano 7:2140–2155. https://doi.org/10.1039/d0en00507j

32. Weekley CM, Aitken JB, Vogt S, Finney LA, Paterson DJ, De Jonge MD, Howard DL, Musgrave IF, Harris HH (2011) Uptake, distribution, and speciation of selenoamino acids by human cancer cells: X-ray absorption and fluorescence methods. Biochemistry

50:1641–1650. https://doi.org/10.1021/bi101678a

33. Lenz M, Van Hullebusch ED, Farges F, Nikitenko S, Borca CN, Grolimund D, Lens PNL (2008) Selenium speciation assessed by X-ray absorption spectroscopy of sequentially extracted anaerobic biofilms. Environ Sci Technol 42:7587–7593. https://doi.org/10.1021/es800811q

34. Chasteen TG (1993) Confusion between dimethyl selenenyl sulfide and dimethyl selenone released by bacteria. Appl Organomet Chem 7:335–342. https://doi.org/10.1002/aoc.590070507

35. Chasteen TG, Bentley R (2003) Biomethylation of selenium and tellurium: Microorganisms and plants. Chem Rev 103:1–25. https://doi.org/10.1021/cr010210+

36. Van Fleet-Stalder V, Chasteen TG, Pickering IJ, George GN, Prince RC (2000) Fate of selenate and selenite metabolized by Rhodobacter sphaeroides. Appl Environ Microbiol 66:4849–4853. https://doi.org/10.1128/AEM.66.11.4849-4853.2000

37. Brady JM, Tobin JM, Gadd GM (1996) Volatilization of selenite in aqueous medium by a Penicillium species. Mycol Res 100:955–961. https://doi.org/10.1016/S0953-7562(96)80048-7

38. Rosenfeld CE, Kenyon JA, James BR, Santelli CM (2017) Selenium (IV,VI) reduction and tolerance by fungi in an oxic environment. Geobiology 15:441–452. https://doi.org/10.1111/gbi.12224

39. Vriens B, Behra R, Voegelin A, Zupanic A, Winkel LHE (2016) Selenium Uptake and Methylation by the Microalga Chlamydomonas reinhardtii. Environ Sci Technol 50:711–720. https://doi.org/10.1021/acs.est.5b04169

40. Fan TWM, Lane AN, Higashi RM (1997) Selenium biotransformations by a euryhaline

microalga isolated from a saline evaporation pond. Environ Sci Technol 31:569–576. https://doi.org/10.1021/es960471e

41. Lindblow-Kull C, Kull FJ, Shrift A (1980) Evidence for the biosynthesis of selenobiotin. Biochem Biophys Res Commun 93:572–576

42. Cherin P, Unger P (1967) The crystal structure of trigonal selenium. Inorg Chem 6:1589–1591. https://doi.org/10.1021/ic50054a037

43. Poborchii V V., Kolobov A V., Oyanagi H, Romanov SG, Tanaka K (1997) Structure of selenium incorporated into nanochannels of mordenite: Dependence on ion exchange and method of incorporation. Chem Phys Lett 280:10–16. https://doi.org/10.1016/S0009-2614(97)01086-5

44. Oremland RS, Herbel MJ, Blum JS, Langley S, Beveridge TJ, Ajayan PM, Sutto T, Ellis A V., Curran S (2004) Structural and Spectral Features of Selenium Nanospheres Produced by Se-Respiring Bacteria. Appl Environ Microbiol 70:52–60. https://doi.org/10.1128/AEM.70.1.52-60.2004

45. Kohara S, Goldbach A, Koura N, Saboungi ML, Curtiss LA (1998) Vibrational frequencies of small selenium molecules. Chem Phys Lett 287:282–288. https://doi.org/10.1016/S0009-2614(98)00184-5

46. Goldan AH, Li C, Pennycook SJ, Schneider J, Blom A, Zhao W (2016) Molecular structure of vapor-deposited amorphous selenium. J Appl Phys 120:. https://doi.org/10.1063/1.4962315

47. Tugarova A V., Mamchenkova P V., Dyatlova YA, Kamnev AA (2018) FTIR and Raman spectroscopic studies of selenium nanoparticles synthesised by the bacterium Azospirillum thiophilum. Spectrochim Acta - Part A Mol Biomol Spectrosc 192:458–

463. https://doi.org/10.1016/j.saa.2017.11.050

48. Mooradian A, Wright GB (1969) THE RAMAN SPECTRUM OF TRIGONAL, $α$-MONOCLINIC AND AMORPHOUS SELENIUm

49. Brodsky MH, Gambino RJ, Smith JE, Yacoby Y (1972) The Raman Spectrum of Amorphous Tellurium. Phys Status Solidi 52:609–614. https://doi.org/10.1002/pssb.2220520229

50. Poborchii V, Kolobov A, Oyanagi H, Romanov S, Tanaka K (1998) Raman and x-ray absorption study of selenium incorporated into the channels of mordenite: dependence on the ion exchange and the method of incorporation. Nanostructured Mater 10:427–436. https://doi.org/10.1016/S0965-9773(98)00083-X

51. Wang T, Yang L, Zhang B, Liu J (2010) Extracellular biosynthesis and transformation of selenium nanoparticles and application in H2O2 biosensor. Colloids Surfaces B Biointerfaces 80:94–102. https://doi.org/10.1016/j.colsurfb.2010.05.041

52. Lucovsky G (1967) Identification of the Fundamental Vibrational Modes. 5:113–117

53. Poborchii V V. (1996) Polarized raman and optical absorption spectra of the mordenite single crystals containing sulfur, selenium, or tellurium in the one-dimensional nanochannels. Chem Phys Lett 251:230–234. https://doi.org/10.1016/0009-2614(96)00045-0

54. Eswayah AS, Smith TJ, Gardiner PHE (2016) Microbial transformations of selenium species of relevance to bioremediation. Appl Environ Microbiol 82:4848–4859. https://doi.org/10.1128/AEM.00877-16

55. Lindblom SD, Wangeline AL, Valdez Barillas JR, Devilbiss B, Fakra SC, Pilon-Smits EAH (2018) Fungal endophyte alternaria tenuissima can affect growth and selenium

accumulation in its hyperaccumulator host astragalus bisulcatus. Front Plant Sci 9:1–12. https://doi.org/10.3389/fpls.2018.01213

56. Schröder I, Rech S, Krafft T, Macy JM (1997) Purification and characterization of the selenate reductase from Thauera selenatis. J Biol Chem 272:23765–23768. https://doi.org/10.1074/jbc.272.38.23765

57. Yee N, Ma J, Dalia A, Boonfueng T, Kobayashi DY (2007) Se(VI) reduction and the precipitation of Se(0) by the facultative bacterium Enterobacter cloacae SLD1a-1 are regulated by FNR. Appl Environ Microbiol 73:1914–1920. https://doi.org/10.1128/AEM.02542-06

58. Kieliszek M, Błażejak S, Gientka I, Bzducha-Wróbel A (2015) Accumulation and metabolism of selenium by yeast cells. Appl Microbiol Biotechnol 99:5373–5382. https://doi.org/10.1007/s00253-015-6650-x

59. Doran JW (1982) Microorganisms and the Biological Cycling of Selenium

Figure legends

Fig 1: Mycelium of *P. blakesleeanus* reduces sodium selenite to SeNPs. a) 28 h old mycelium of *P. blakesleeanus* supplemented with 2 mM and 10 mM Se^{+4} and incubated for 24 h, C-control; **b)** Separated mycelium and growth medium from Fig 1a; **c)** Washed mycelium from Fig 1a**; d)** fresh medium (M), filtrate of 28 h old mycelium (F) and boiled 28 h old mycelium (BM) supplemented with 10 mM Se^{+4} and incubated for 7 days

Fig 2. SEM (up) and EDS (down) of a) 28 h old mycelia and b) mycelial exudate treated with 10 mM Se^{+4} for 24 h. SeNPs are indicated by arrows.

Fig 3. Size distribution of SeNPs produced by mycelium of 28 h old *P.blakesleeanus* measured by DLS method. Distribution, given as a function of size vs number of SeNPs in exudate of mycelium, reveals the SeNPs diameter range from 32 to 95 nm.

Fig 4. XANES spectra of *P. blakesleeanus* mycelium treated with Se^{+4}. a) reference standards of Se^0 (black), Se^{+4} (blue) vs. mycelium incubated with 0.5 mM Se^{+4} for 24h (green); **b)** the first derivative spectra of Se^0 reference standard and the mycelium treated with Se^{+4} after 1h from treatment; **c)** mycelium incubated with 0.5 mM Se^{+4} for 1h (orange), 3h (purple and 24 h (green); **d)** mycelium incubated with 10 mM Se^{+4} for 24 h (red) vs reference standards of Se^0 (black) and Se^{+4} (blue); **e)** the first derivative spectra of Se^0, Se^{+4} and DMSe reference standards vs mycelium treated for 24 h with 10 mM Se^{+4}; **f)** the first derivative spectra of mycelium treated for 1h, 3h and 24 h with 10 mM Se^{+4}.

Fig 5. Raman spectra of *P blakesleeaus* treated with 10 mM Se^{+4} for 28 h. a) spectra of mycelium (green) with most intensive band at 255 cm^{-1}, characteristic for vibrational bands of SeNPs, and soluble fraction (red) with broad band at 354 cm^{-1}, most probably derived from the intracellular interaction between Se and sulfur containing protein components; **b)** deconvolution of main mycelial band at 255 cm^{-1} reveals predominantly monoclinic Se_8 chains, together with trigonal Se polymer chain, Se_8 and Se_6 ring structures.

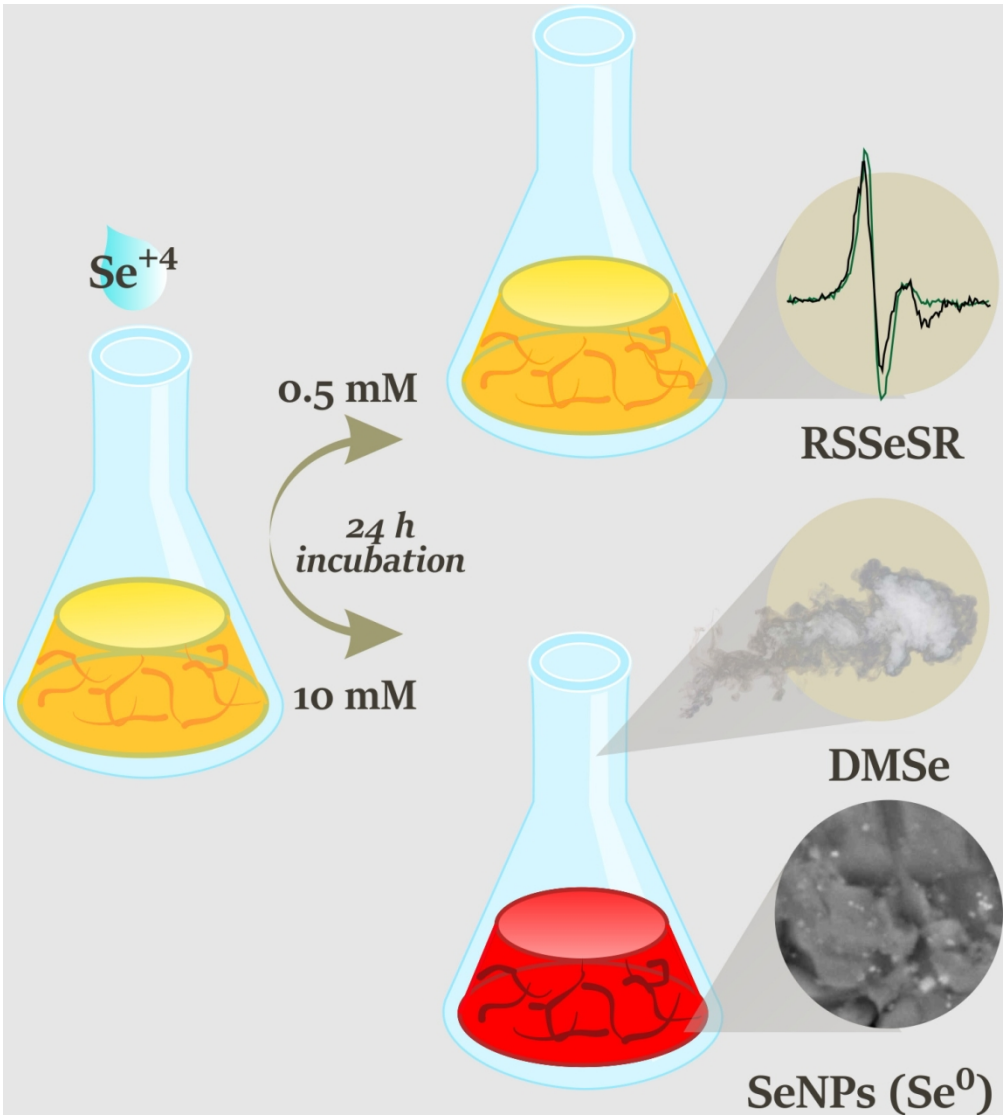
Se+4
0.5 mM
24 h
incubation
10 mM
RSSeSR
DMSe
SeNPs (Se0)

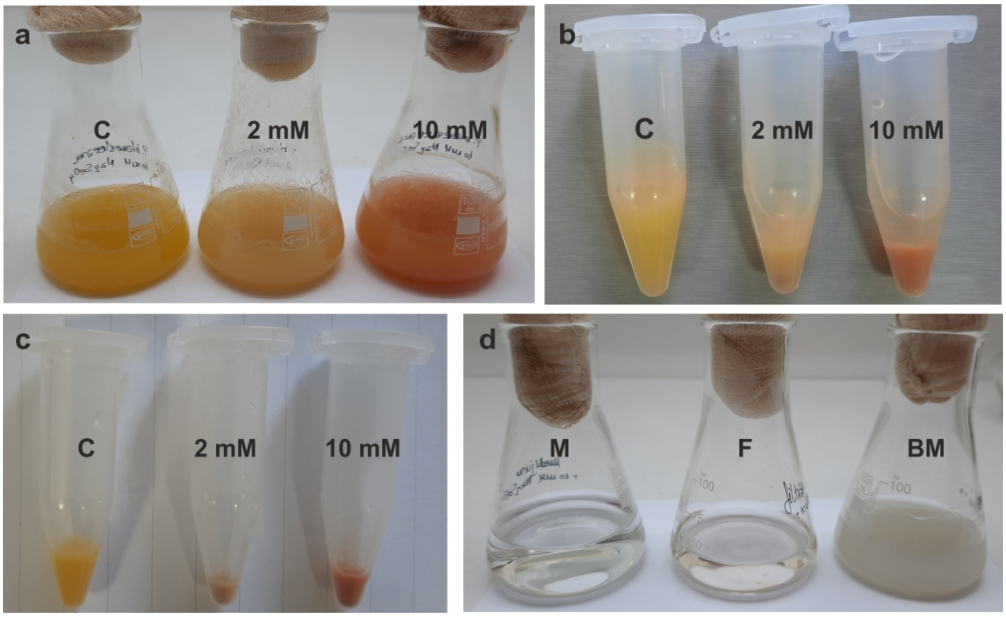

Fig 1: Mycelium of P. blakesleeanus reduces sodium selenite to SeNPs. a) 28 h old mycelium of P. blakesleeanus supplemented with 2 mM and 10 mM Se+4 and incubated for 24 h, C-control; b) Separated mycelium and growth medium from Fig 1a; c) Washed mycelium from Fig 1a; d) fresh medium (M), filtrate of 28 h old mycelium (F) and boiled 28 h old mycelium (BM) supplemented with 10 mM Se+4 and incubated for 7 days.

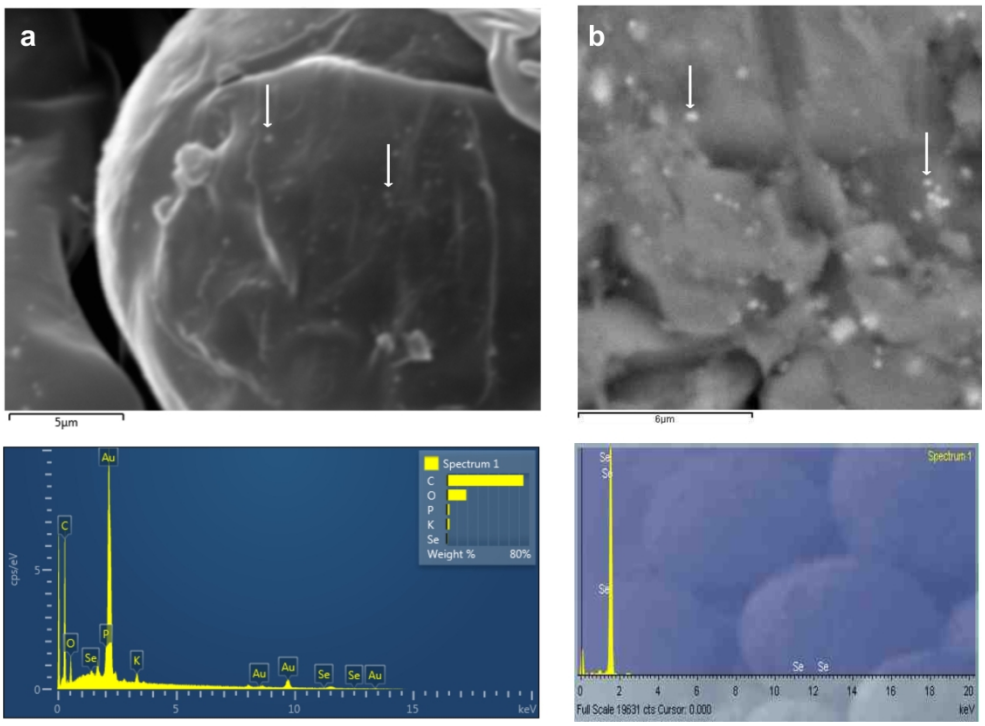

Fig 2. SEM (up) and EDS (down) of a) 28 h old mycelia and b) mycelial exudate treated with 10 mM Se+4 for 24 h. SeNPs are indicated by arrows.

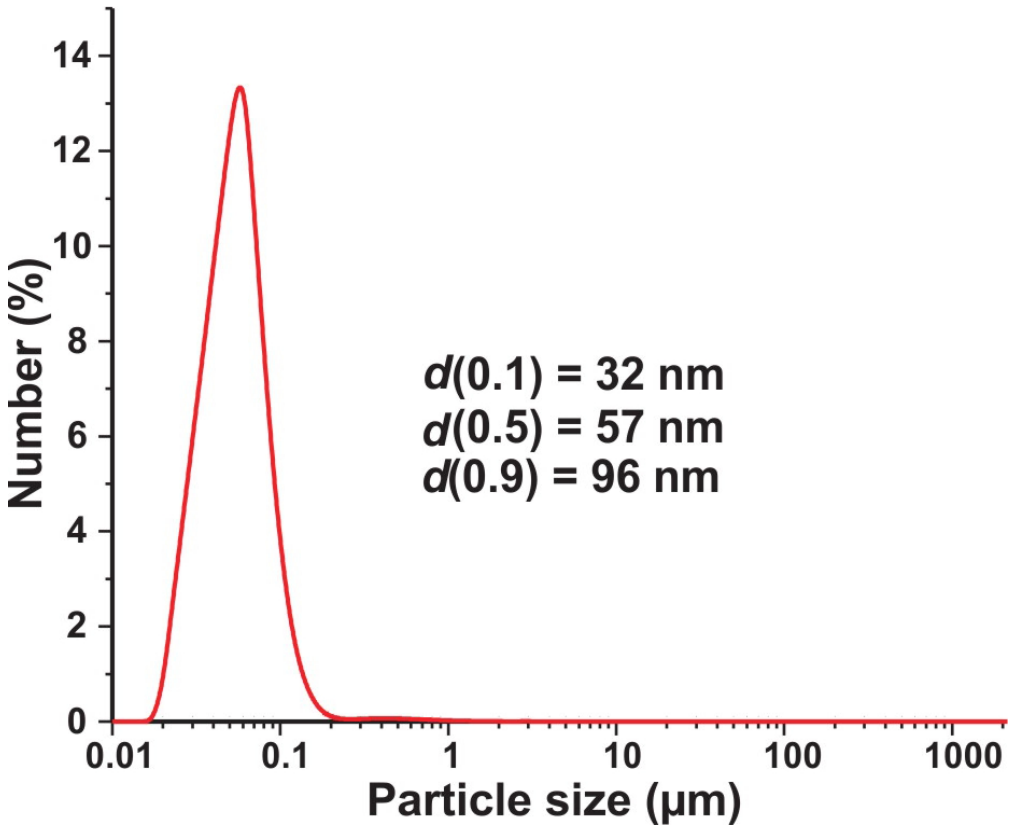

Fig 3. Size distribution of SeNPs produced by mycelium of 28 h old P.blakesleeanus measured by DLS method. Distribution, given as a function of size vs number of SeNPs in exudate of mycelium, reveals the SeNPs diameter range from 32 to 95 nm.

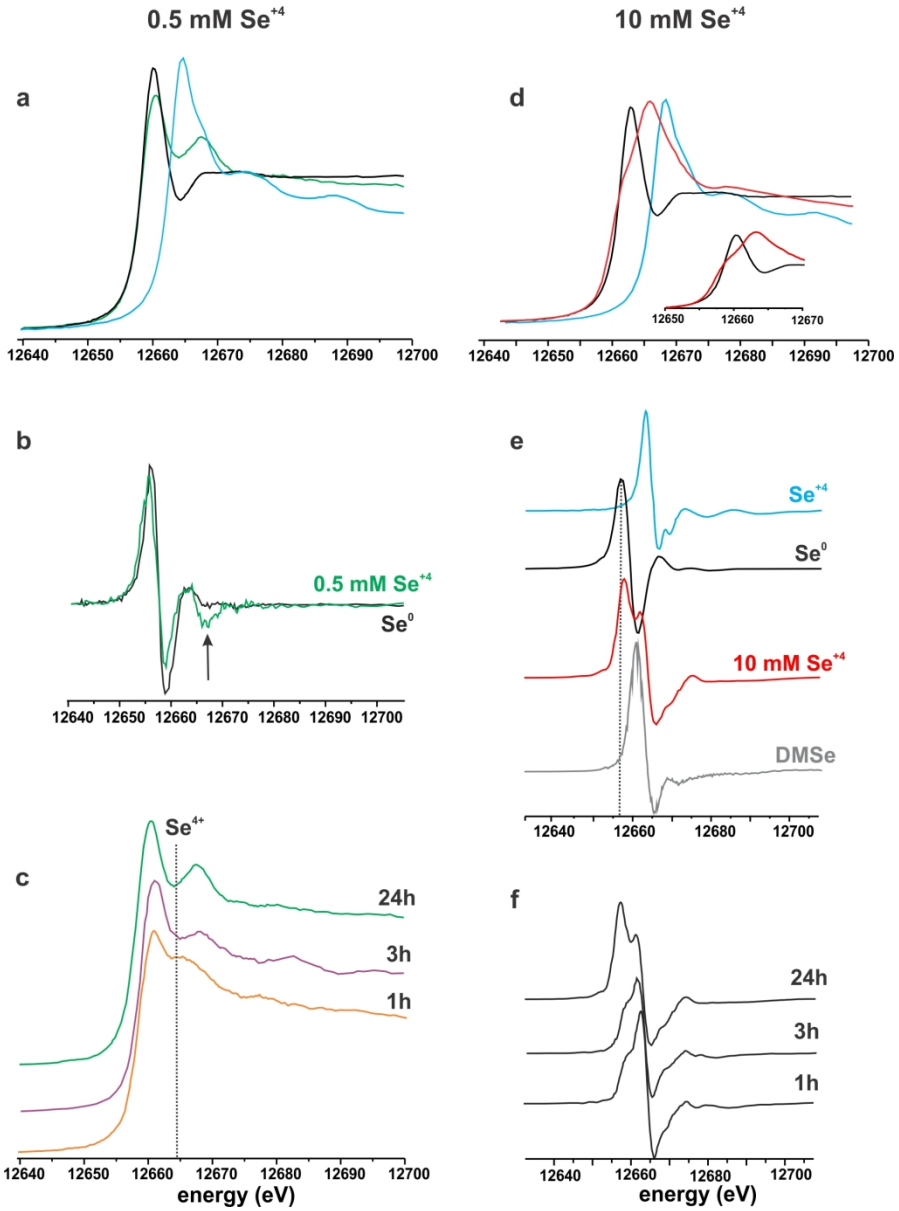

Fig 4. XANES spectra of P. blakesleeanus mycelium treated with Se+4. a) reference standards of Se0 (black), Se+4 (blue) vs. mycelium incubated with 0.5 mM Se+4 for 24 h (green); b) the first derivative spectra of Se0 reference standard and the mycelium treated with Se+4 after 1h from treatment; c) mycelium incubated with 0.5 mM Se+4 for 1h (orange), 3h (purple and 24 h (green); d) mycelium incubated with 10 mM Se+4 for 24 h (red) vs reference standards of Se0 (black) and Se+4 (blue); e) the first derivative spectra of Se0, Se+4 and DMSe reference standards vs mycelium treated for 24 h with 10 mM Se+4; f) the first derivative spectra of mycelium treated for 1h, 3h and 24 h with 10 mM Se+4.

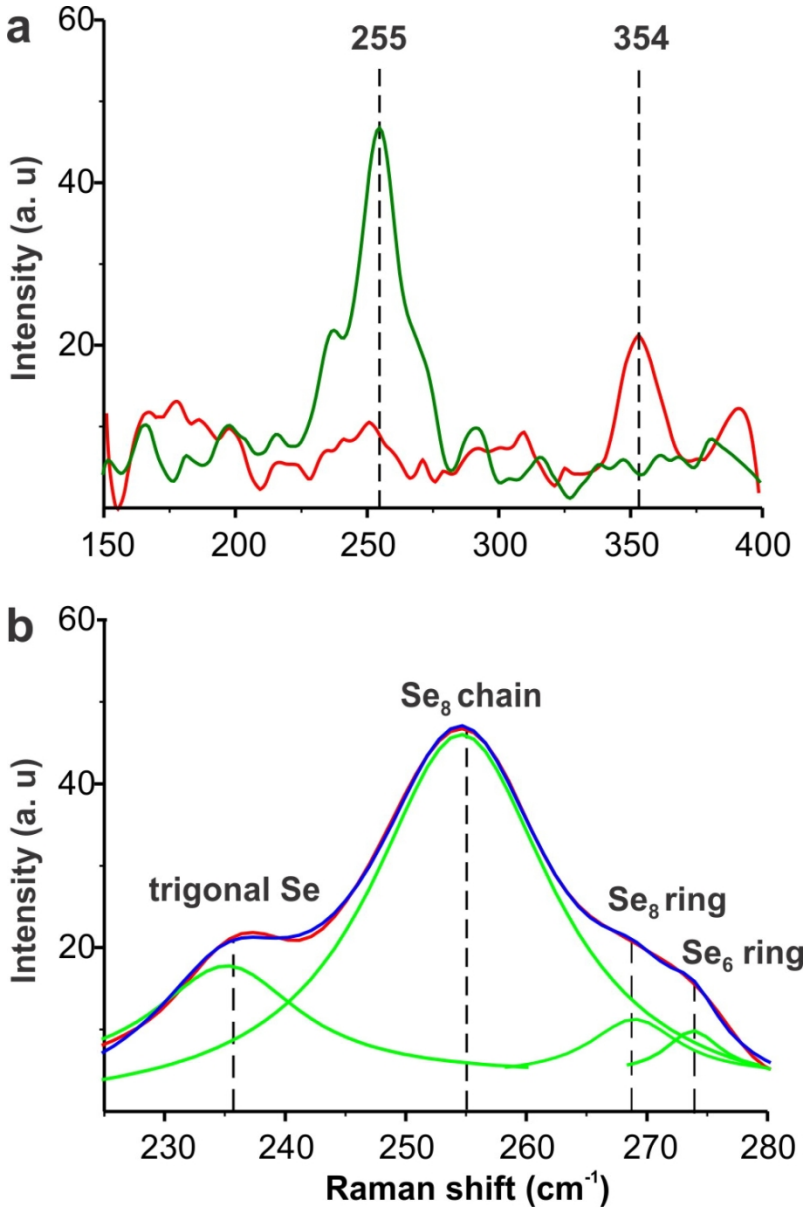

Fig 5. Raman spectra of P blakesleeaus treated with 10 mM Se+4 for 28 h. a) spectra of mycelium (green) with most intensive band at 255 cm-1, characteristic for vibrational bands of SeNPs, and soluble fraction (red) with broad band at 354 cm-1, most probably derived from the intracellular interaction between Se and sulfur containing protein components; b) deconvolution of main mycelial band at 255 cm-1 reveals predominantly monoclinic Se8 chains, together with trigonal Se polymer chain, Se8 and Se6 ring structures.